nonlinear :)

Novel Metrics for Time Series Analysis of Accreting Systems

Rebecca A Phillipson (she/her)

MPS-Ascend Postdoctoral Fellow

rebecca.phillipson@villanova.edu

@raphillipson

@beckastrosaurus

UIUC The Transient and Variable Universe

❖ June 21st, 2023

NSF Award Number: 2138155

VILLANOVA UNIVERSITY

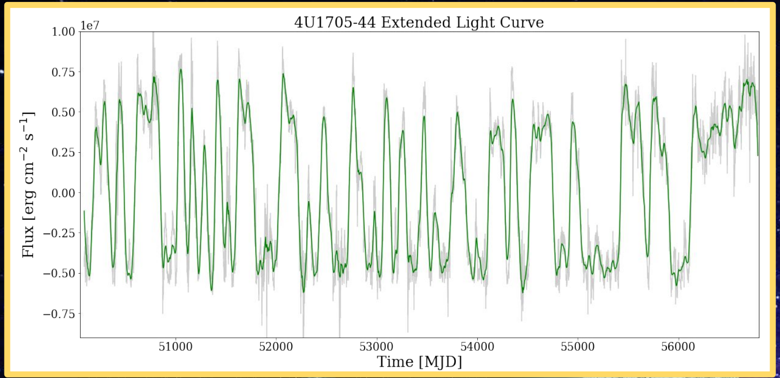
4U1705-44 Extended Light Curve
1e7
Flux [erg cm^{-2} s^{-1}]
Time [MJD]
1.00
0.75
0.50
0.25
0.00
−0.25
−0.50
−0.75
51000
52000
53000
54000
55000
56000

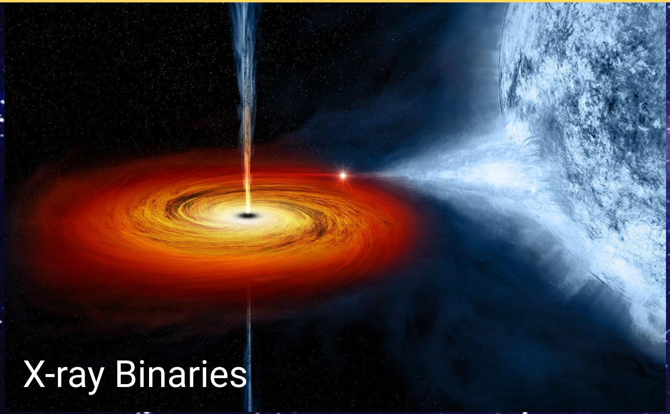
X-ray Binaries

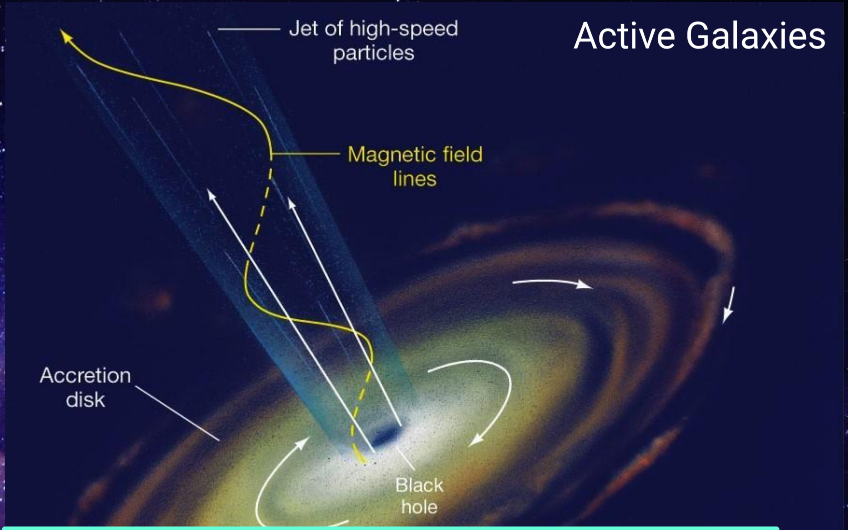
Active Galaxies
Jet of high-speed particles
Magnetic field lines
Accretion disk
Black hole

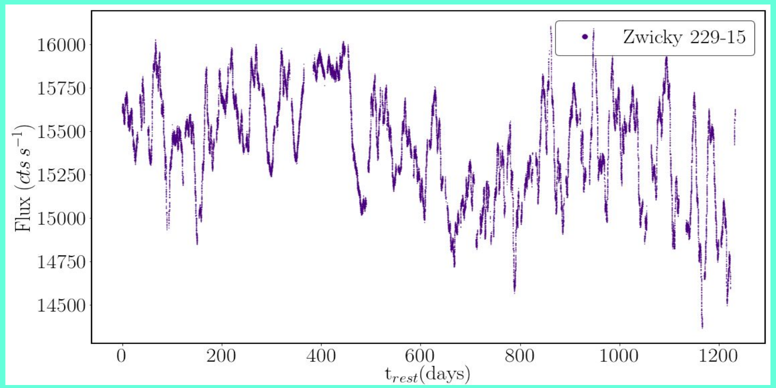
Zwicky 229-15
Flux ($cts\ s^{-1}$)
t_{rest}(days)
16000
15750
15500
15250
15000
14750
14500
0
200
400
600
800
1000
1200

GRS 1915+105: Black Hole X-ray Binary

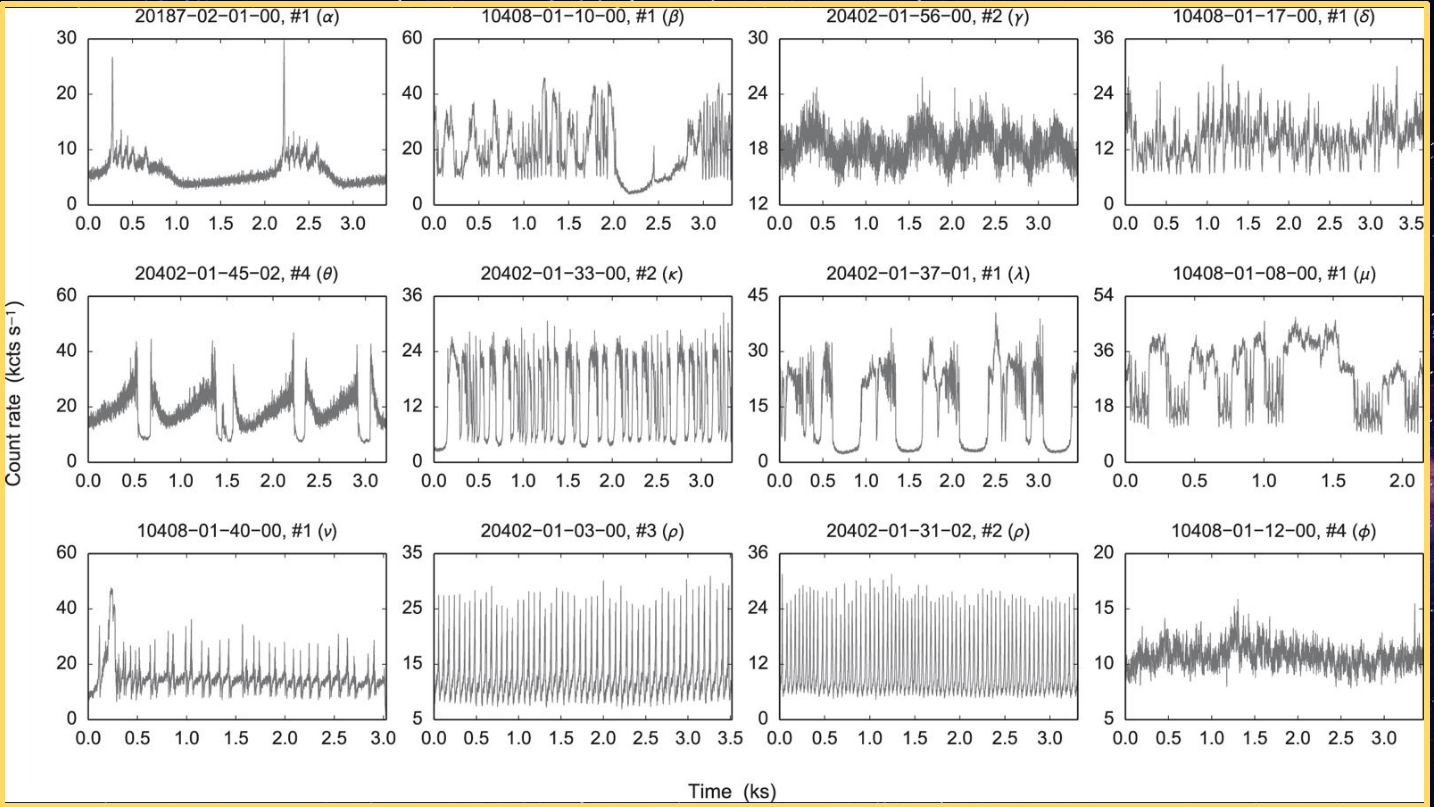

Mannattil, Gupta, and Chakraborty 2016

GRS 1915+105: Black Hole X-ray Binary

Mannattil, Gupta, and Chakraborty 2016

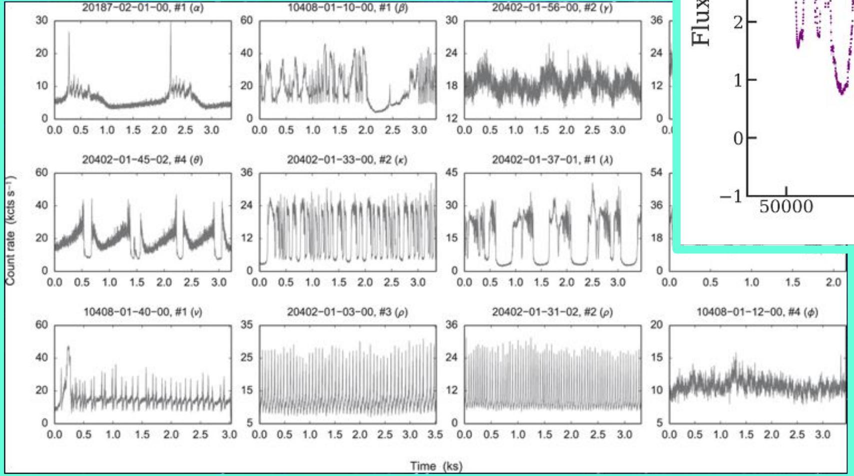

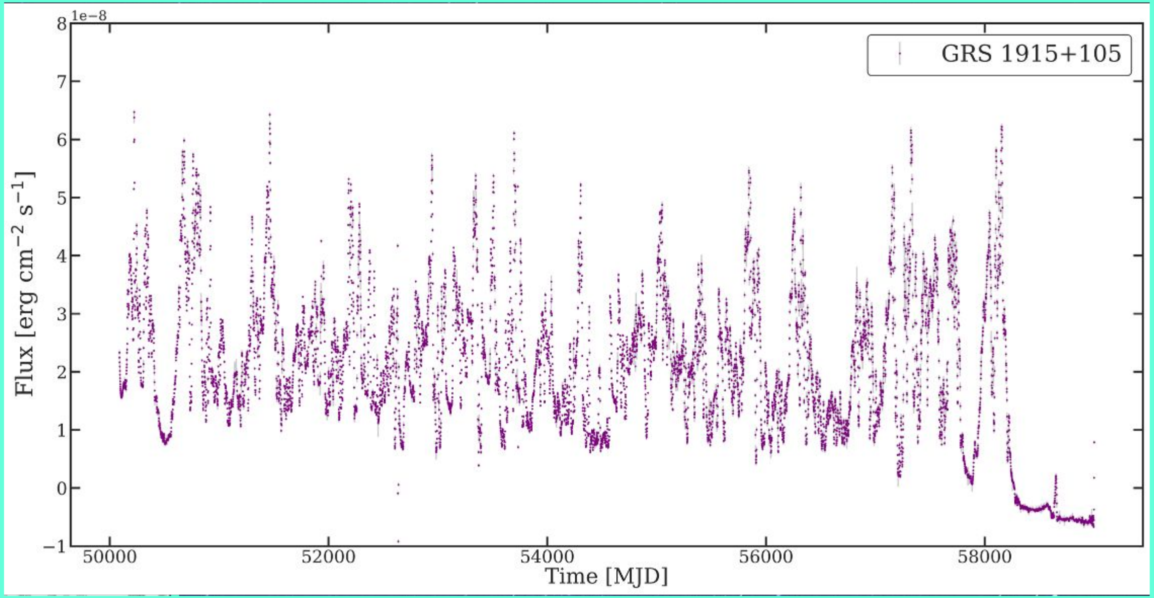

Phillipson 2020

GRS 1915+105: Black Hole X-ray Binary

Unpredictable
Self-similar
Recurrent but not periodic

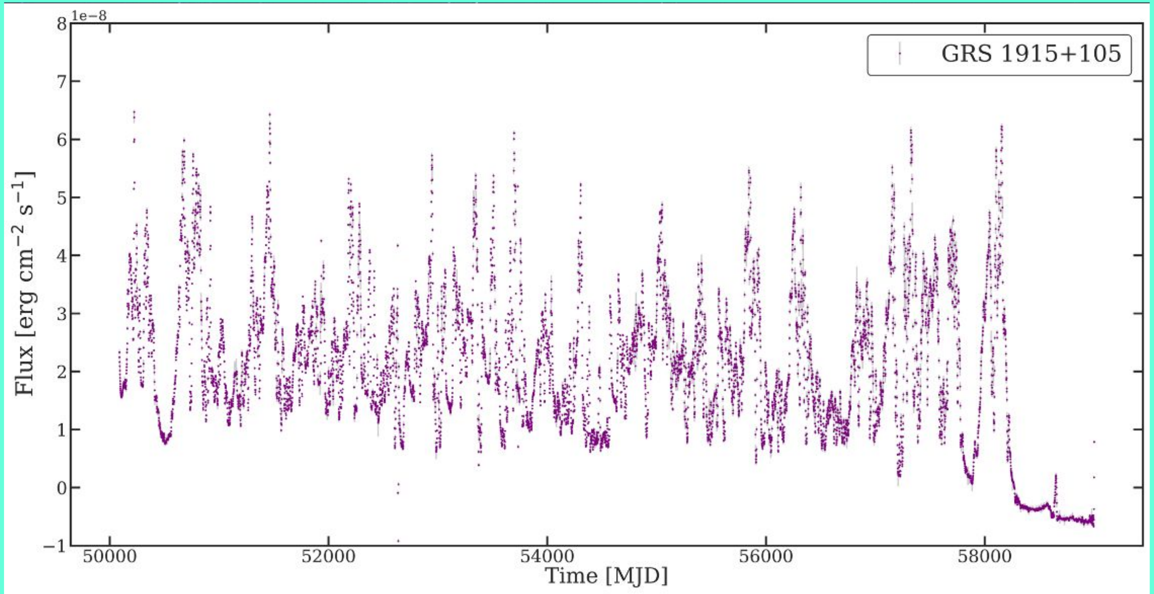

Phillipson 2020

Mannattil, Gupta, and Chakraborty 2016

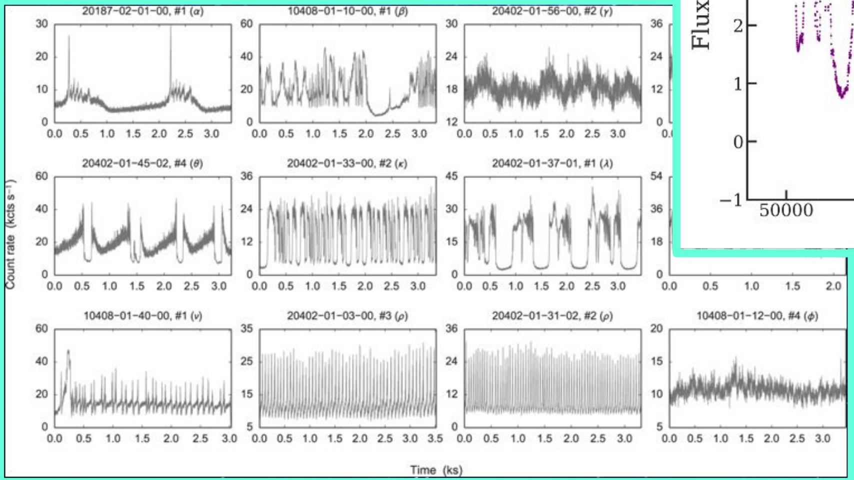

Uncovering Dynamics from Time Series

Hyperion: satellite of Saturn

- Wisdom, Peale, and Mignard (1984) predicted it exhibits chaotic rotation
- The time evolution of the angle between the long axis and a reference:

$$\frac{d^2\theta}{dt^2} + \left(\frac{\omega_0^2}{2r^3}\right)\sin 2(\theta - f) = 0$$

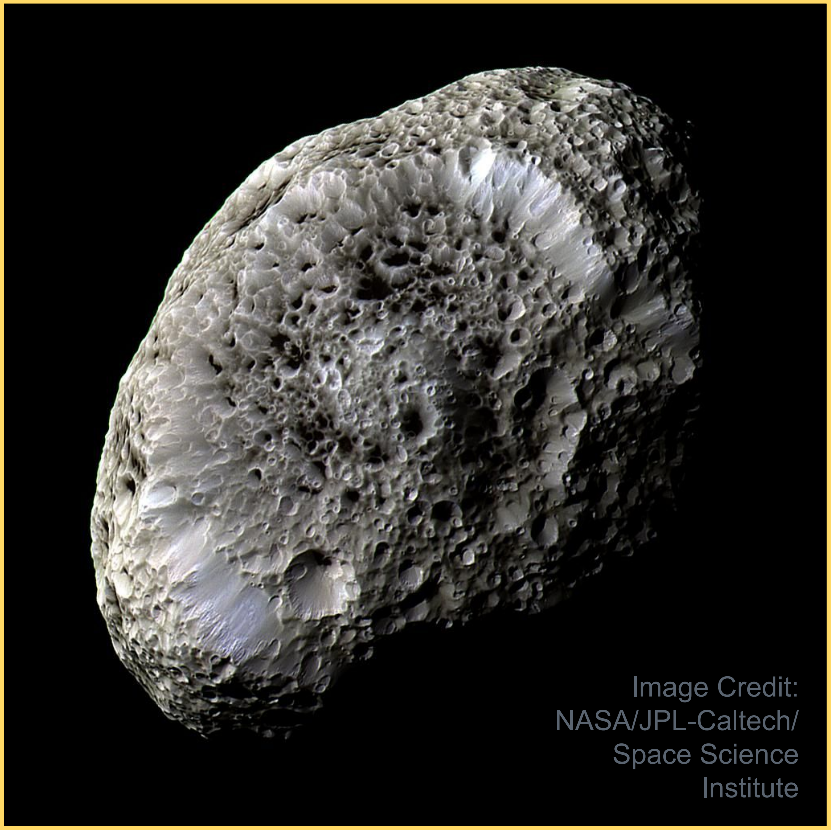

Image Credit: NASA/JPL-Caltech/ Space Science Institute

Uncovering Dynamics from Time Series

Hyperion: satellite of Saturn

- Wisdom, Peale, and Mignard (1984) predicted it exhibits chaotic rotation
- The time evolution of the angle between the long axis and a reference:

$$\frac{d^2\theta}{dt^2} + \left(\frac{\omega_0^2}{2r^3}\right)\sin 2(\theta - f) = 0$$

- The irregular rotation, shape, and reflectivity leads the brightness of Hyperion to also be chaotic
- Klavetter (1989) made time series measurements of Hyperion's brightness and confirmed chaos

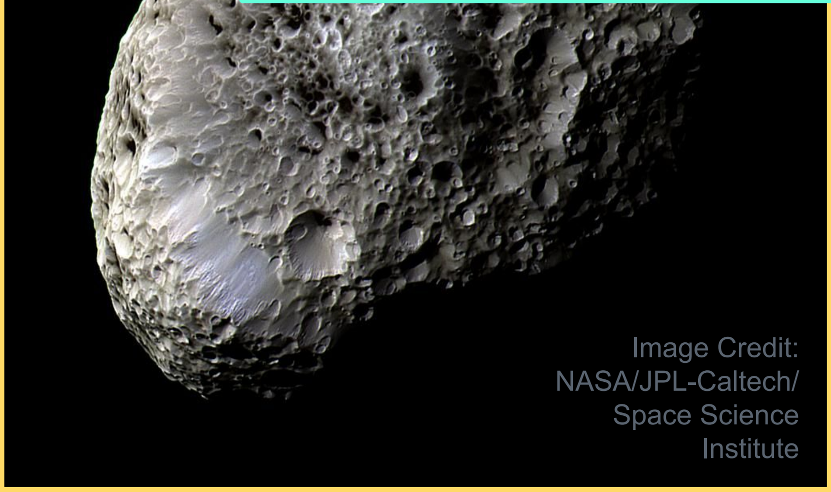

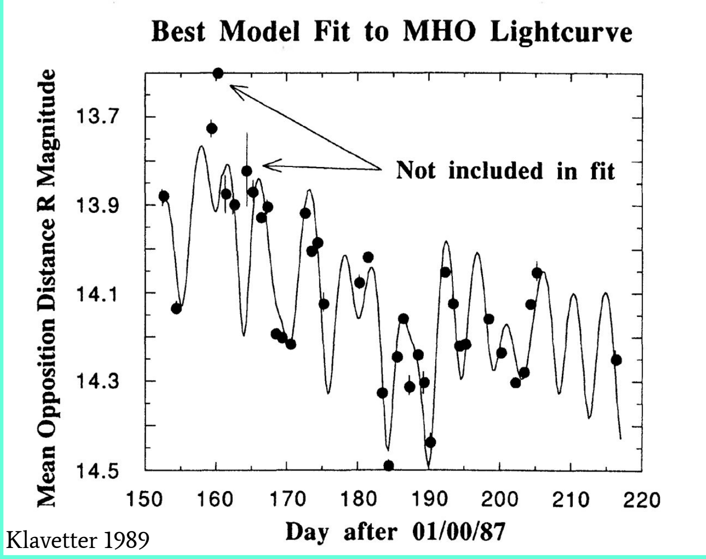

Klavetter 1989

Uncovering Dynamics from Time Series

Variable Stars: R Scuti

- R Scuti is an aperiodic pulsating star
- Buchler et al. (1996) calculated a low fractal dimension (D=3.1) and a positive Lyapunov exponent, strong indications of chaos

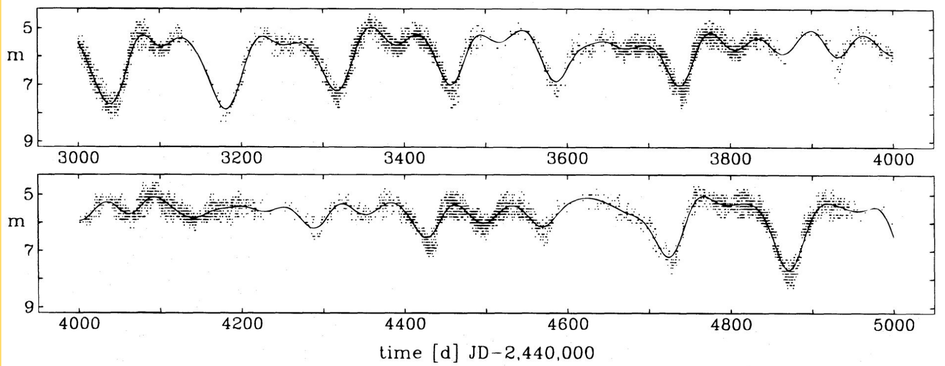

FIG. 1.—Typical observed light curve segments for R Scuti. *Dots:* the individual observations; *line:* the smoothed filtered signal.

Uncovering Dynamics from Time Series

Variable Stars: R Scuti

- R Scuti is an aperiodic pulsating star
- Buchler et al. (1996) calculated a low fractal dimension (D=3.1) and a positive Lyapunov exponent, strong indications of chaos
- Buchler et al. (2004) then applied the same technique to other semi-regular pulsating stars: R UMi, RS Cyg, V CVn, and UX Dra
- Dynamics of the stars take place in a 4D space: two vibrational modes involved in the pulsation

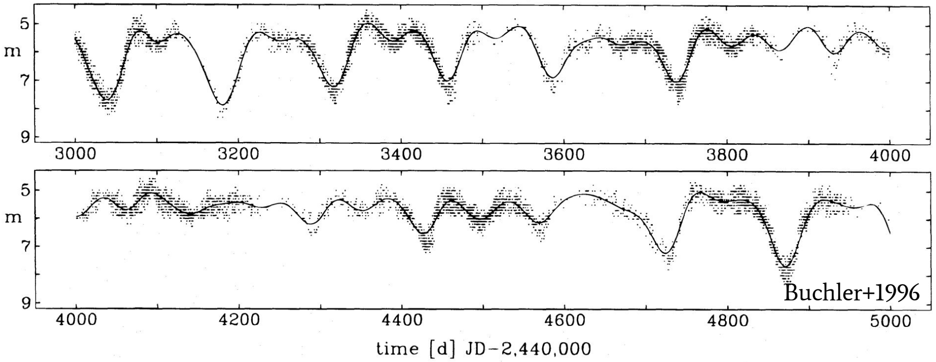

FIG. 1.—Typical observed light curve segments for R Scuti. *Dots*: the individual observations; *line*: the smoothed filtered signal.

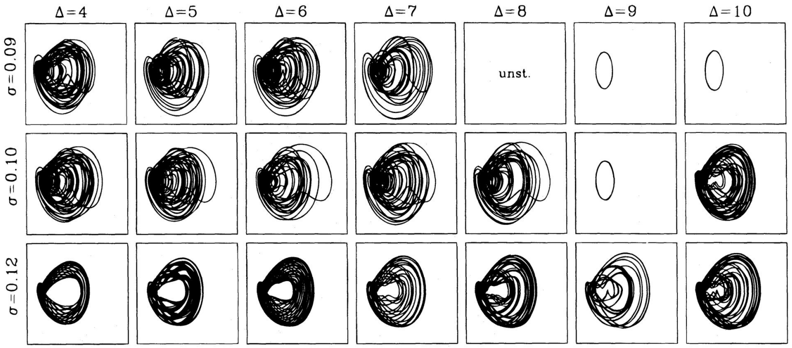

FIG. 7.—Lowest BK projections (four-dimensional maps) for different values of Δ and σ_s

Buchler+2004

Uncovering Dynamics from Time Series

What about variable accreting sources?

Challenges:

- Number of cycles of fundamental timescales (baseline)
- Quality of data (signal-to-noise)
- Sampling of time series (cadence)

Uncovering Dynamics from Time Series

What about variable accreting sources?

Challenges:

- Number of cycles of fundamental timescales (baseline)
- Quality of data (signal-to-noise)
- Sampling of time series (cadence)

Ongoing and upcoming instruments (somewhat) relieve these challenges:

- X-ray All-Sky Monitors (RXTE, MAXI) have provided *long* time series
- Improved sensitivity (NICER, STROBE-X)
- Use of optical exoplanet missions for other science: Kepler, TESS
- The abundance of data from ground-based observatories: ZTF, LSST

A Brief Detour: The Logistic Map

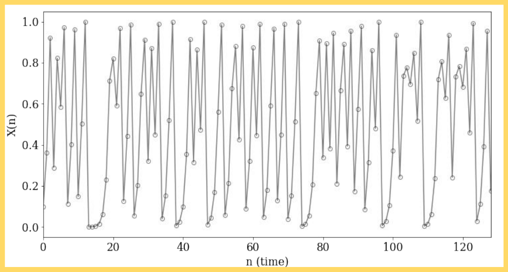

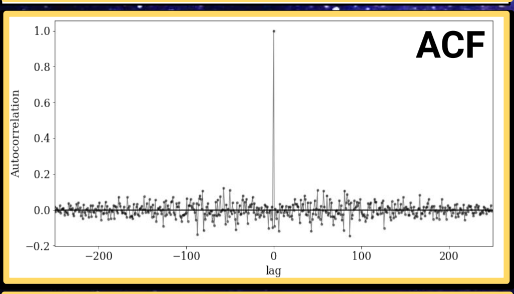

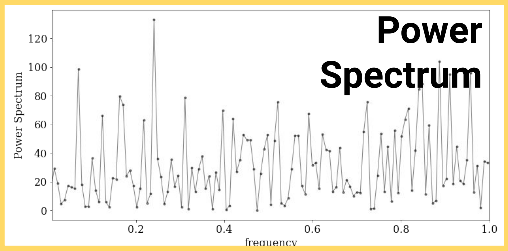

- The **Logistic Map**, from population studies:

$$X_{n+1} = f(X_n) = \lambda X_n(1 - X_n)$$

- It is **deterministic**, but for certain parameter values (λ=4), it is maximally chaotic.

A Brief Detour: The Logistic Map

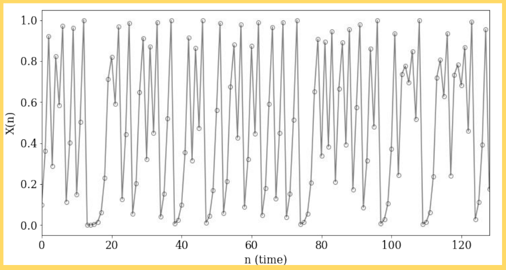

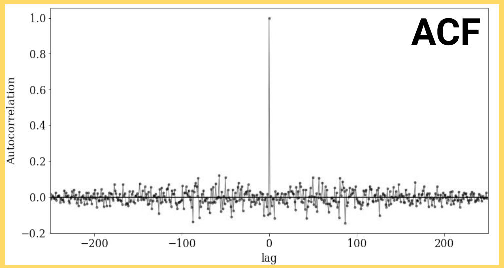

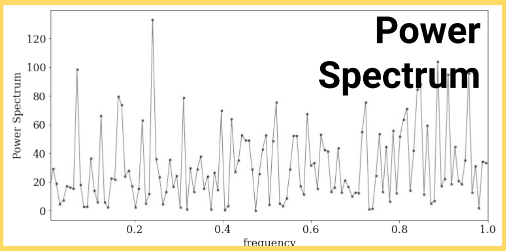

- The **Logistic Map**, from population studies:

$$X_{n+1} = f(X_n) = \lambda X_n (1 - X_n)$$

- It is **deterministic**, but for certain parameter values (λ=4), it is maximally chaotic
- Autocorrelations and power spectrum are indistinguishable from white noise

White Noise

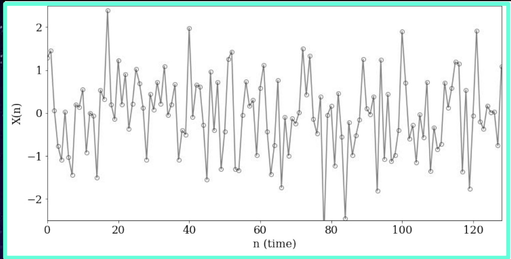

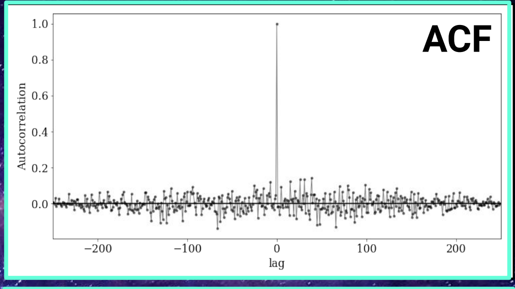

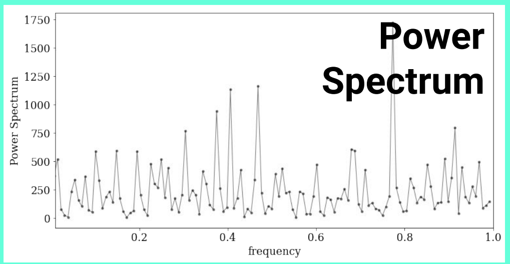

A Brief Detour: The Logistic Map

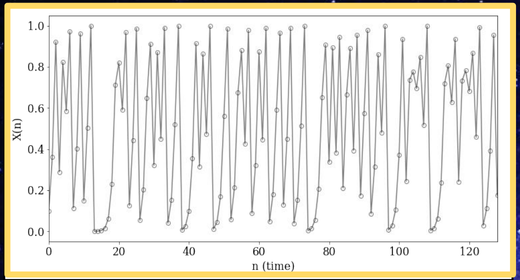

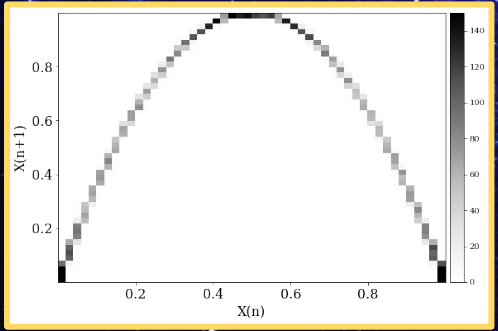

- The **Logistic Map**, from population studies:

$$X_{n+1} = f(X_n) = \lambda X_n(1 - X_n)$$

- It is **deterministic**, but for certain parameter values (λ=4), it is maximally chaotic
- Autocorrelations and power spectrum are indistinguishable from white noise
- If X were random, then all points X_n would be independent of each other → Joint Probability Distribution
- *See Scargle 2009 (Encyclopedia of Complexity and Systems Science) for detailed review of this topic.*

White Noise

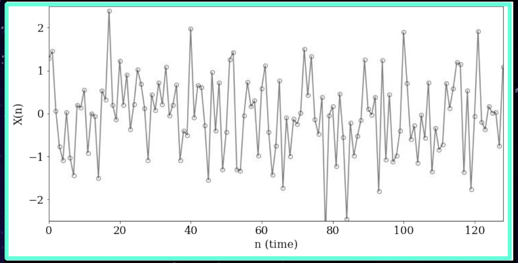

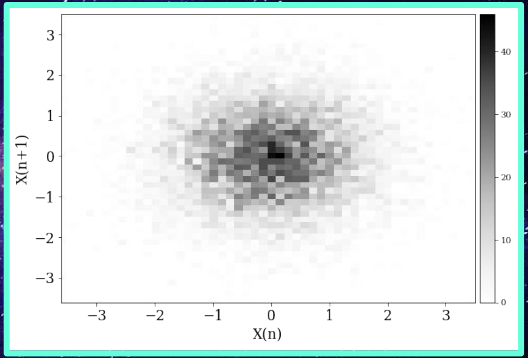

A Brief Detour: The Logistic Map

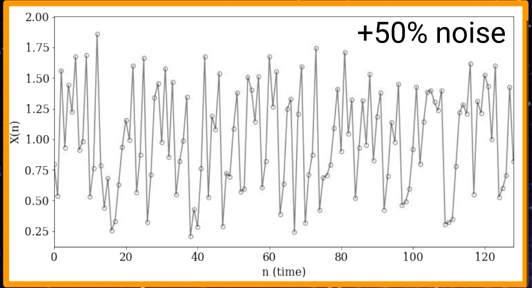

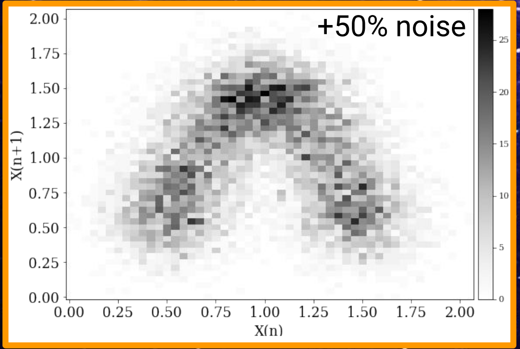

- The **Logistic Map**, from population studies:

$$X_{n+1} = f(X_n) = \lambda X_n(1 - X_n)$$

- It is **deterministic**, but for certain parameter values (λ=4), it is maximally chaotic
- Autocorrelations and power spectrum are indistinguishable from white noise
- If X were random, then all points X_n would be independent of each other → Joint Probability Distribution
- *See Scargle 2009 (Encyclopedia of Complexity and Systems Science) for detailed review of this topic.*

White Noise

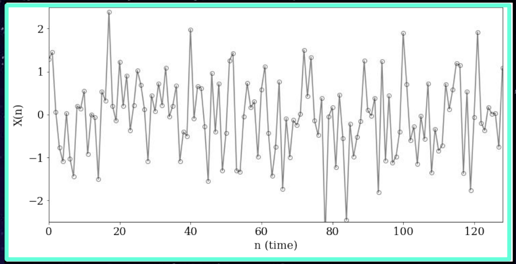

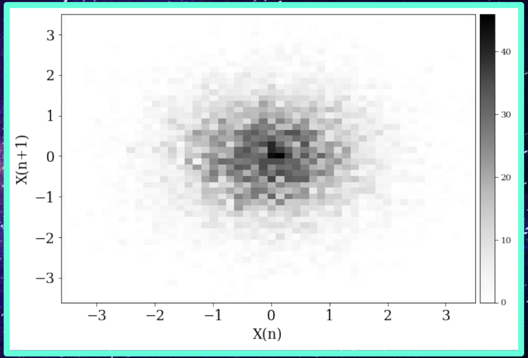

More on Joint Probability Distribution

- Nichols et al. 2009 demonstrates analytically how the ***bispectrum*** can be used to detect deviations from normality in the joint probability distribution of a system
- For a time series divided into K segments, the bispectrum is:

$$B(k,l) = \frac{1}{K}\sum_{i=0}^{K-1} X_i(k)X_i(l)X_i^*(k+l)$$

X(f): the Fourier transform at frequency f

- Reflects the coupling of three frequencies
- **Bicoherence**: the magnitude of the bispectrum
- *See Maccarone (2013) for an overview*

Bispectrum of XRBs

Arur & Maccarone (2023) study GRS 1915+105 and find the bicoherence pattern correlates with the QPO frequency, hardness ratio, and radio properties

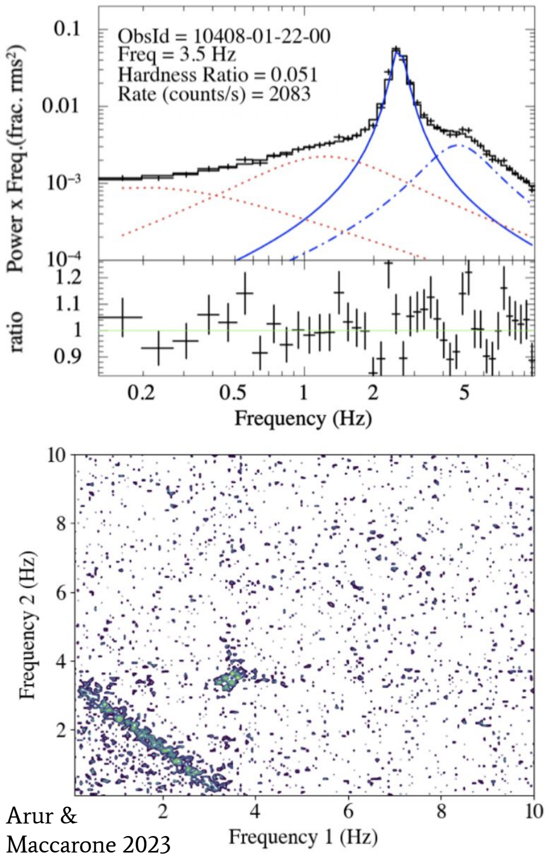

Arur & Maccarone 2023

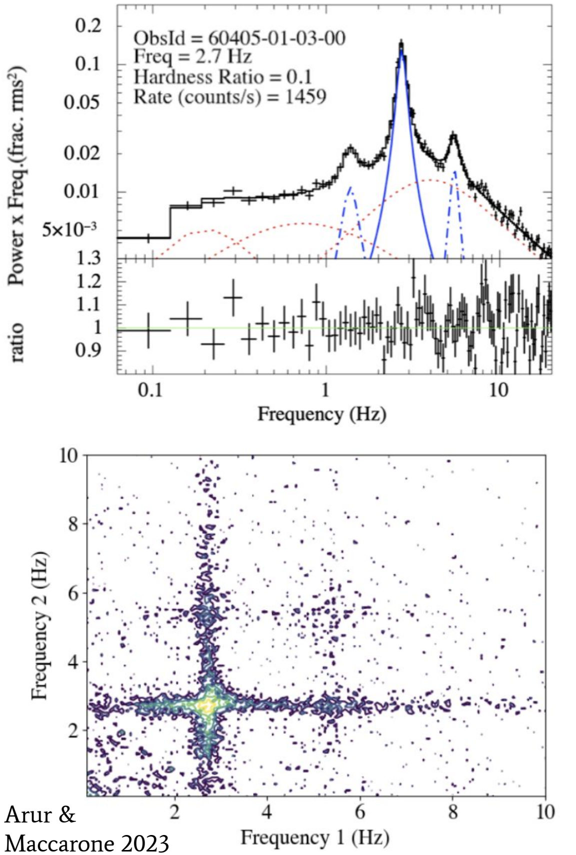

Arur & Maccarone 2023

Bispectrum of XRBs

Arur & Maccarone (2023) study GRS 1915+105 and find the bicoherence pattern correlates with the QPO frequency, hardness ratio, and radio properties

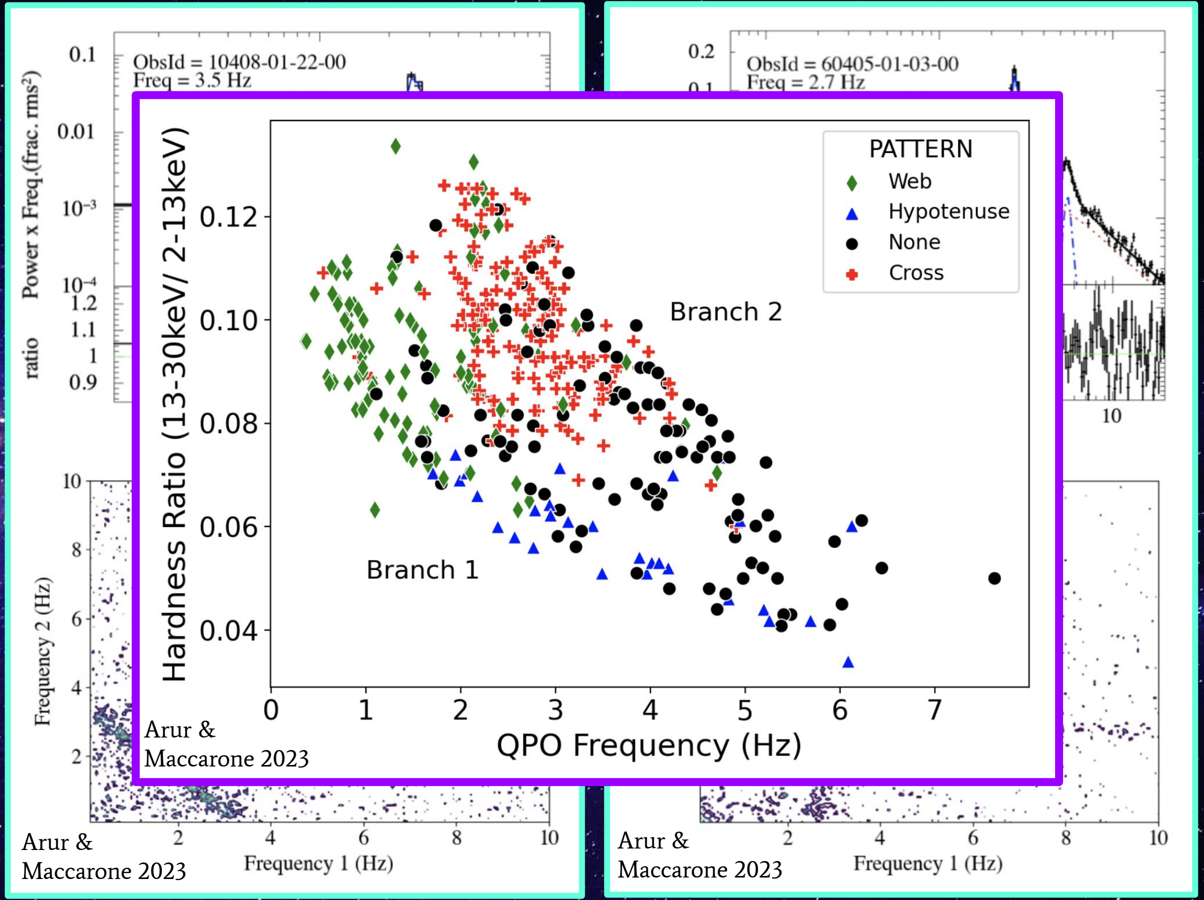

Phase (State) Space

- The **bispectrum** and **bicoherence** describe nonlinearities in a signal and are sensitive to changes in the joint probability distribution of a system
    - **Unfortunately, requires lots of high-quality data**
- The **joint probability distribution** can be represented by X(n) vs. X(n+1) and is distinct from the power spectrum, ACF, etc.
  → **provides relationships between datapoints (not their absolute times)**
- **This feature is related to the importance of phase space (state space)**

Phase Space encodes dynamical information

We can construct phase space from 1D time series:

- Analytical systems: direct derivatives or multivariate

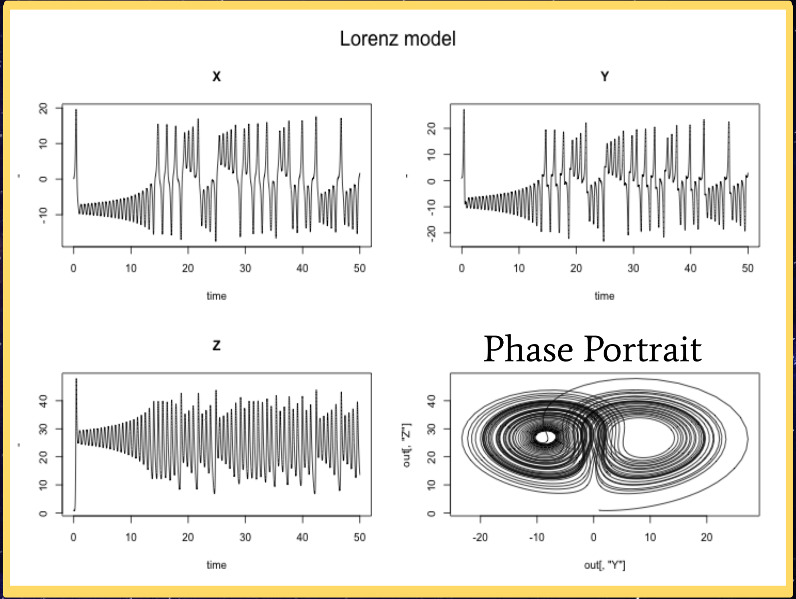

Phase Space encodes dynamical information

We can construct phase space from 1D time serie

- Analytical systems: direct derivatives
- Known observed systems: numerical derivatives

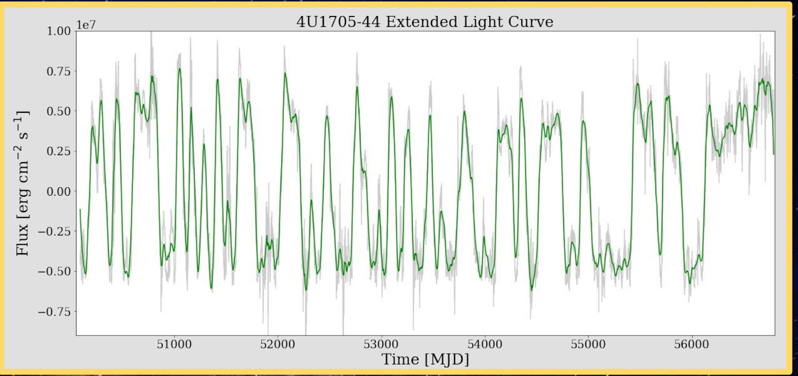

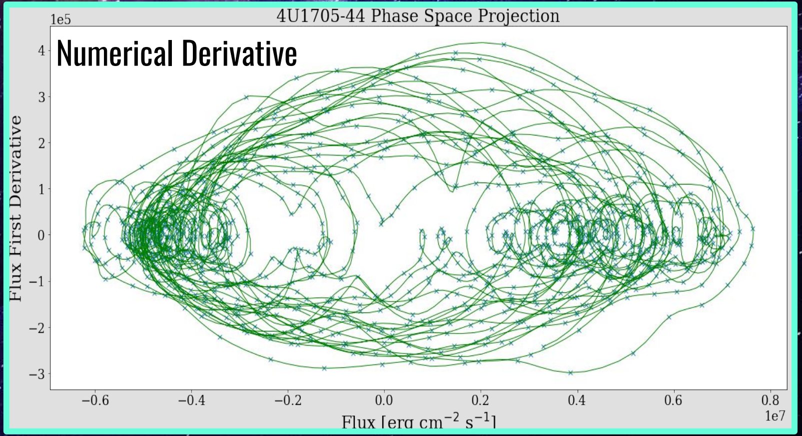

Phase Space encodes dynamical information

We can construct phase space from 1D time series:

- Analytical systems: direct derivatives
- Known observed systems: numerical derivatives
- Unknown observed systems - *most common*: **Time Delay Embedding** (*Takens 1981*)

$$X \to (X_n, X_{n+k}, X_{n+2k}, X_{n+3k} + \cdots + X_{n+(M-1)k})$$

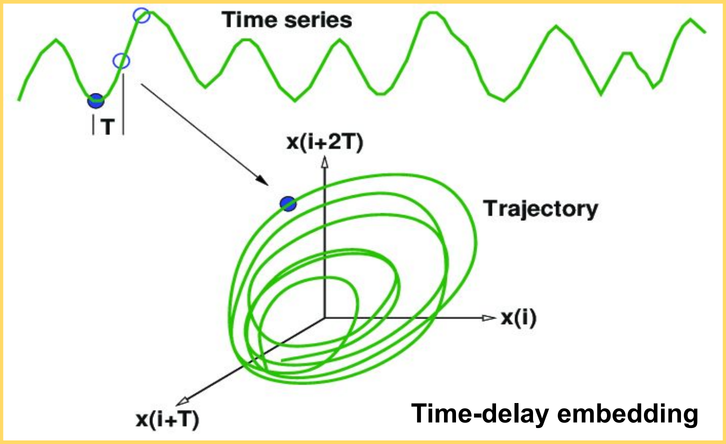

The trajectories in an embedding preserve the dynamics of the true state space (Packard et al. 1980)

Phase Space encodes dynamical information

We can construct phase space from 1D time series:

- Analytical systems: direct derivatives
- Known observed systems: numerical derivatives
- Unknown observed systems - *most common*: Time Delay Embedding (*Takens 1981*)
    - Example: derivative of *sine* = phase-shifted *cosine*
    - Example: 4U1705-44 time delay embedding for a delay of 30 looks like its numerical derivative

- **Phase space in its simplest form is merely X(n) vs. X(n+1)**

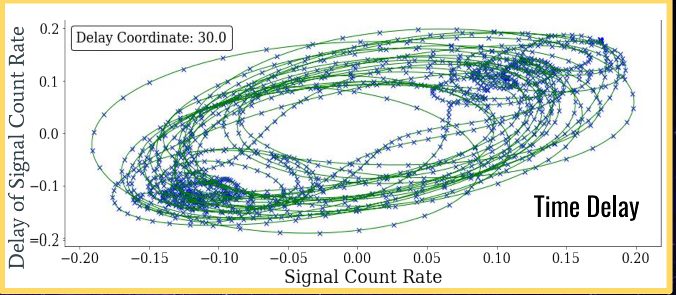

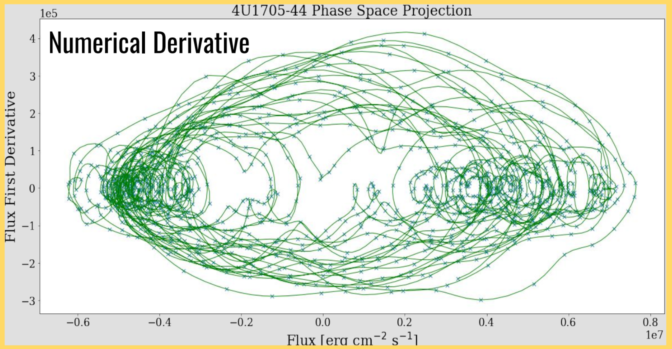

Phase Space encodes dynamical information

Advantages of the phase space framework:

- Robust against noise
- No assumptions about linearity, stationarity, etc.
- Detect transitions to/from nonlinear or periodic regimes
- Methods require less data compared to other nonlinear techniques

The Recurrence Plot:

A One-stop Shop for info contained in Phase Space

- The Recurrence Plot associates positions in time with closeness in phase space

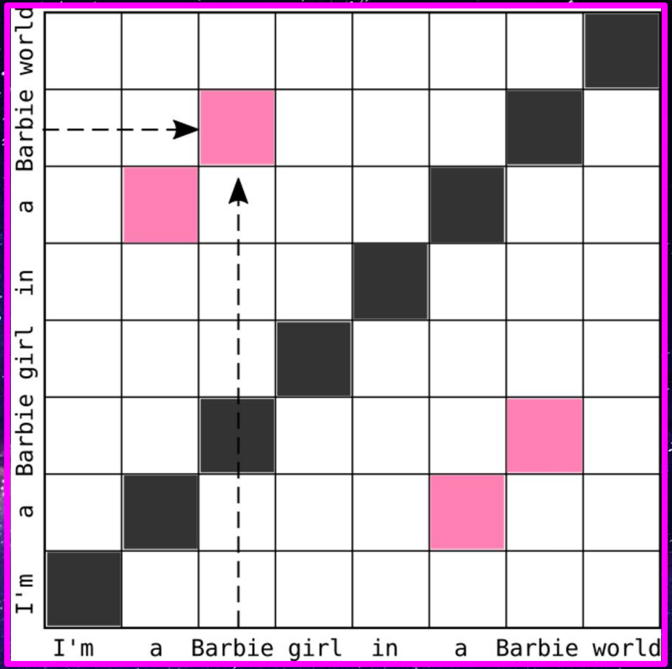

"SongSim":
https://colinmorris.github.io/SongSim

The Recurrence Plot:

A One-stop Shop for information contained in Phase Space

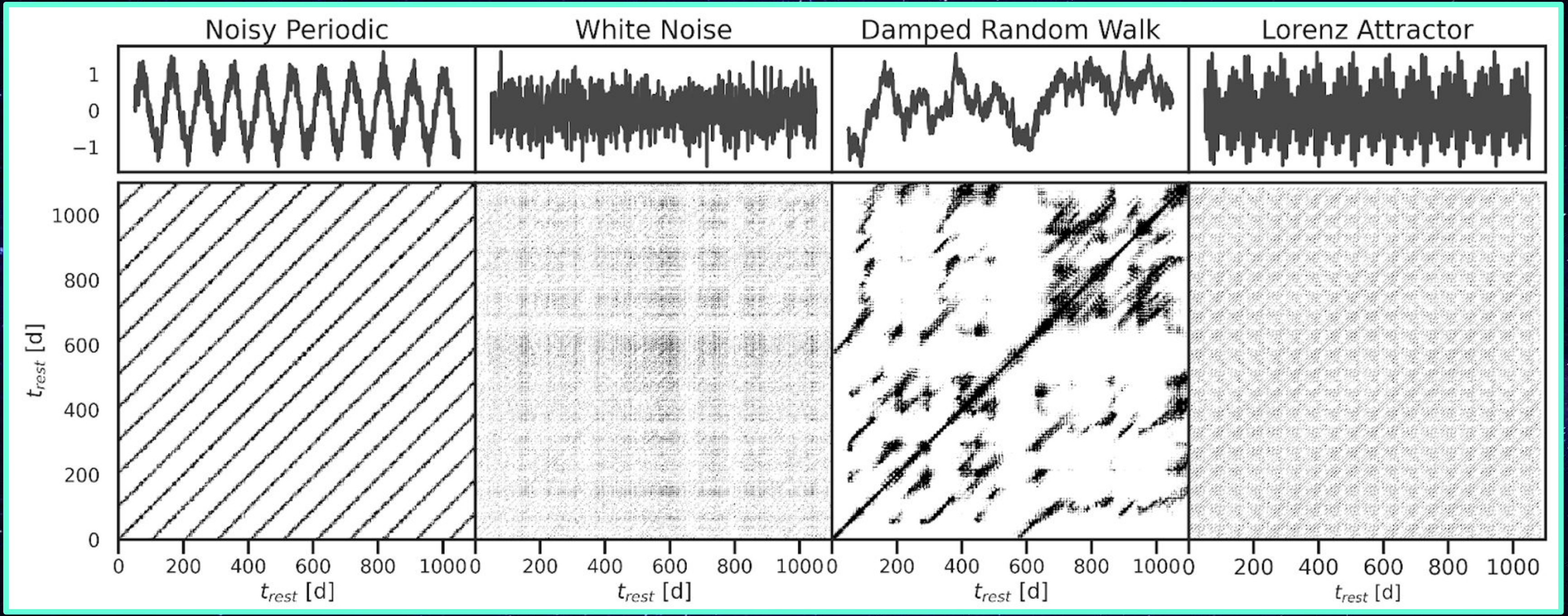

Broadbent & Phillipson 2023 (in review)

The Recurrence Plot:

A One-stop Shop for info contained in Phase Space

- The Recurrence Plot associates positions in time with closeness in phase space
- Can be used with noise-like & deterministic systems

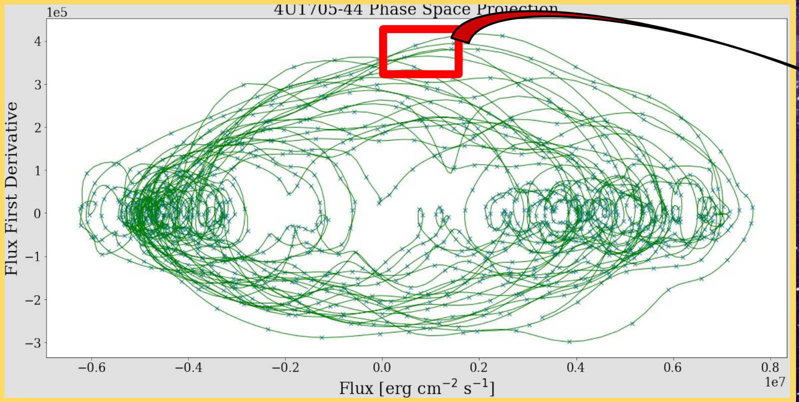

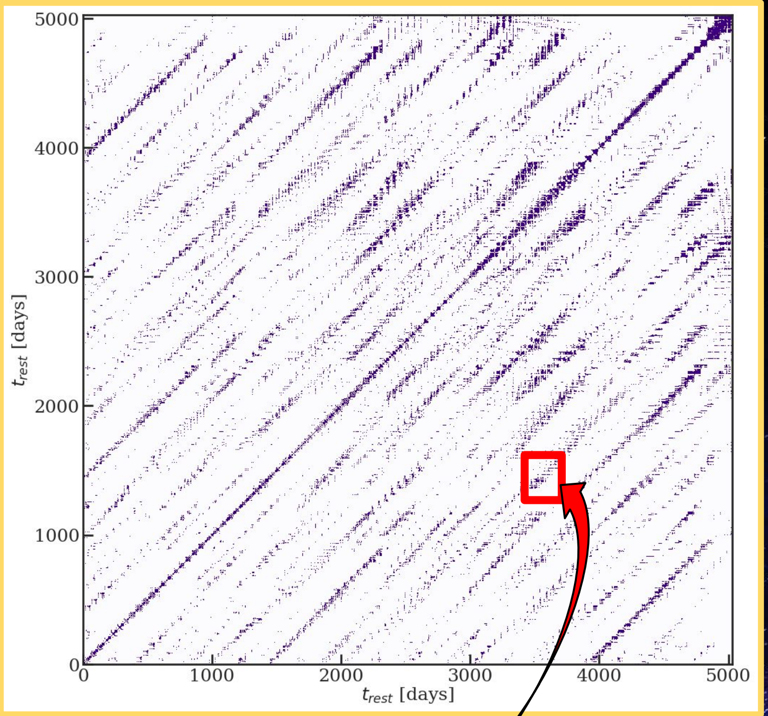

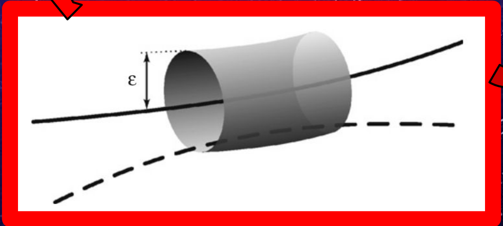

Phillipson et al. 2018

The Recurrence Plot:
X-ray Binaries!

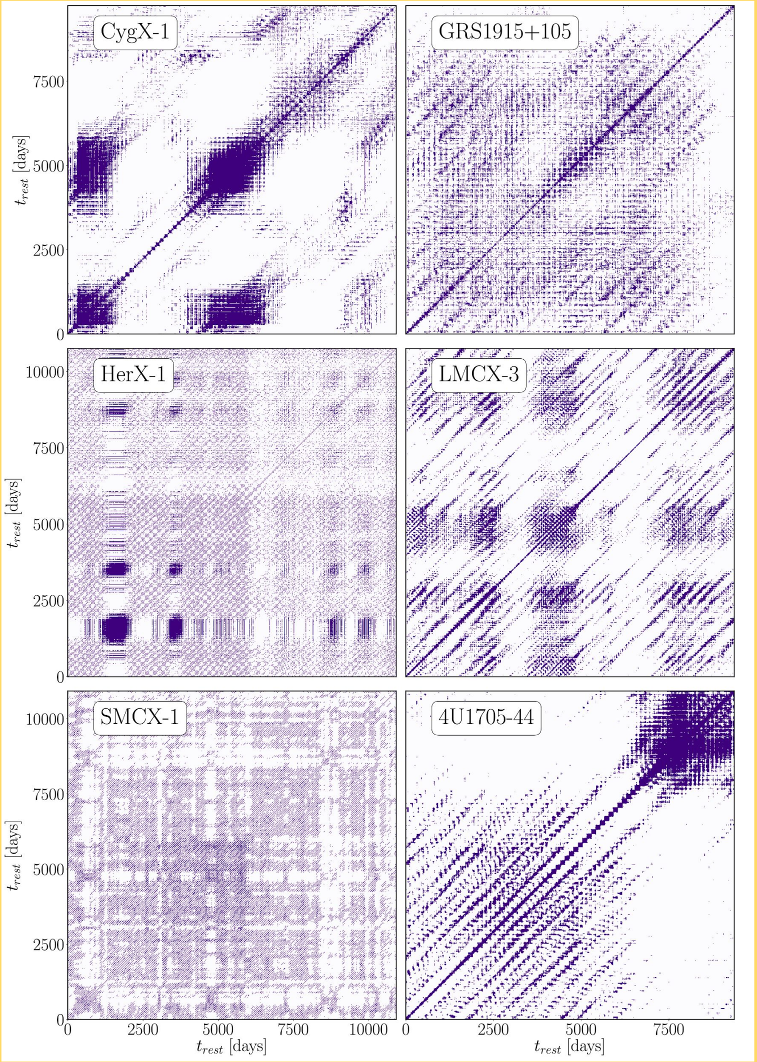

Phillipson et al. 2020

Back to Hyperion

Boyd et al. 1994 used a version of the recurrence plot (RP) to extract unstable periodic orbits responsible for the chaotic behavior.

The method is more robust against noise and supports the Buchler et al. results.

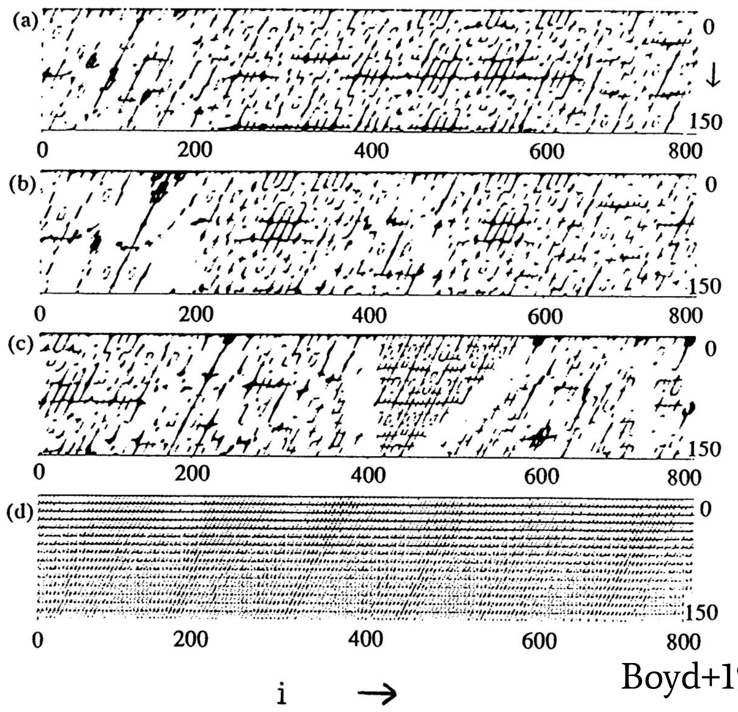

Boyd+1994

FIG. 3.—Close return images for four separate initial conditions of the Hyperion system. The body parameters are fixed, and the initial value of f is taken as zero in each experiment. The initial conditions are (a) $\theta = 1.0$, $\theta' = 0.5$; (b) $\theta = 0.7$, $\theta' = 1.0$; (c) $\theta = 0.5$, $\theta' = 0.5$; and (d) $\theta = 2.0$, $\theta' = 2.0$. The horizontal axis is the position i of a point in the data file that is compared with another point in the data file separated by p nights, with p plotted vertically downward. If the phase-space distance between the two points is less than 10% of the maximum, we plot a black point at (i, p).

The Recurrence Plot for Accretion Studies

- Sukova et al. 2016: identifies determinism and chaos among several variability states of 6 microquasars using RPs relating to thermal-viscous instability

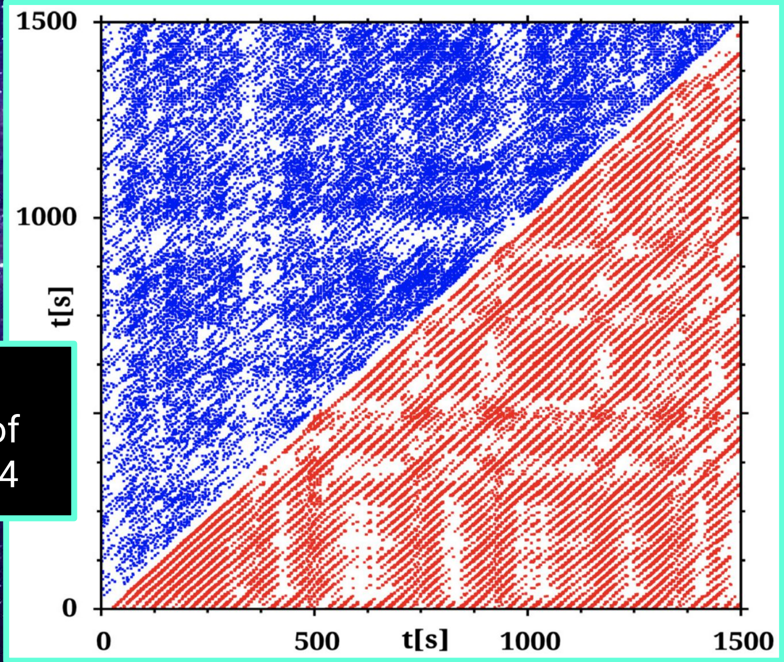

Two different spectral states of IGR J17091-3624

Sukova et al. 2016

The Recurrence Plot for Accretion Studies

- Bhatta et al. 2020: computes RP statistics of blazars and found several with traces of determinism, with most containing a combination of determinism & stochastic processes

The Recurrence Plot for Accretion Studies

- Phillipson et al. 2020: computes the Renyi entropy from the RPs of two Kepler-monitored AGN. One is deterministic (with an optical QPO) and the other is not: two classes of AGN?

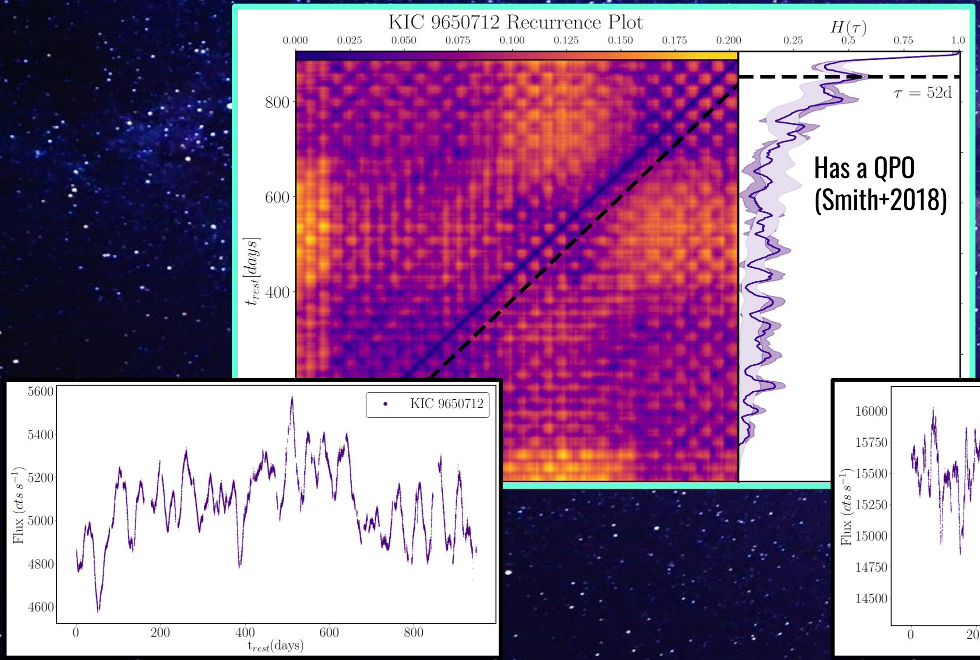

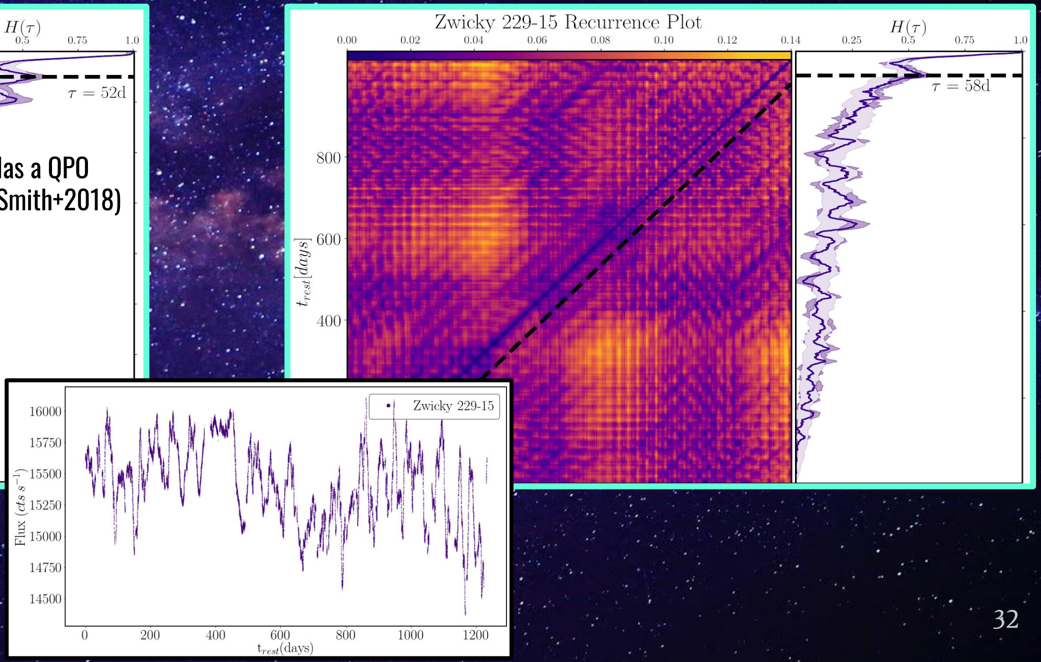

The Recurrence Plot for Accretion Studies

- Phillipson et al. 2023: compute RP statistics of 46 Swift/BAT AGN.
- Type II contain higher measures of determinism relative to Type I, but no distinction is found in obscuration.
- Some dependencies on Eddington ratio.

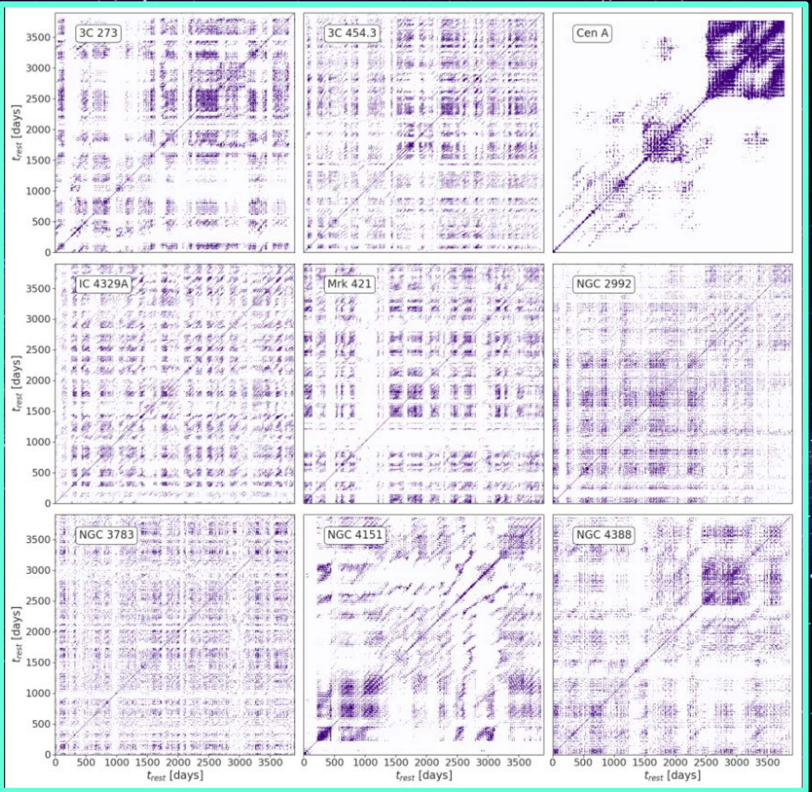

Accretion State Changes of Cyg X-1

Broadbent & Phillipson 2023 (in review)

Data: 2-20 keV Flux, Rossi X-ray Timing Explorer (RXTE) All-sky Monitor (ASM) and MAXI

Cyg X-1: Known to undergo state changes regularly

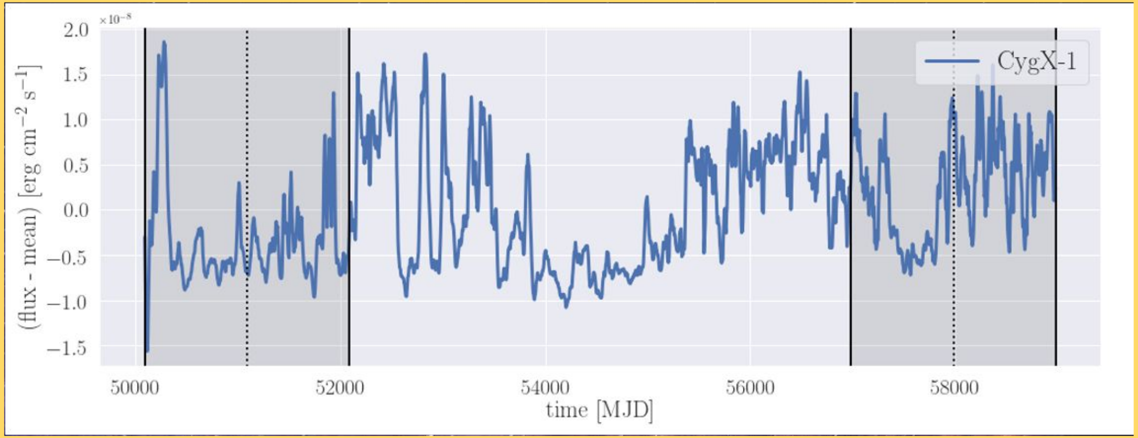

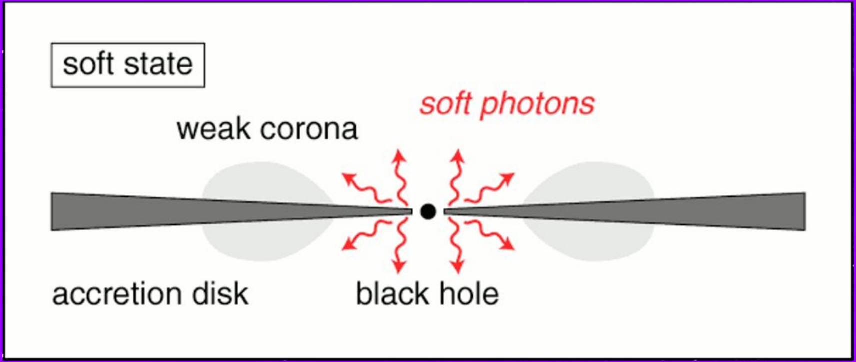

Disk-dominated "soft" state: mostly thermal photons, lower energies

Accretion State Changes of Cyg X-1

Broadbent & Phillipson 2023 (in review)

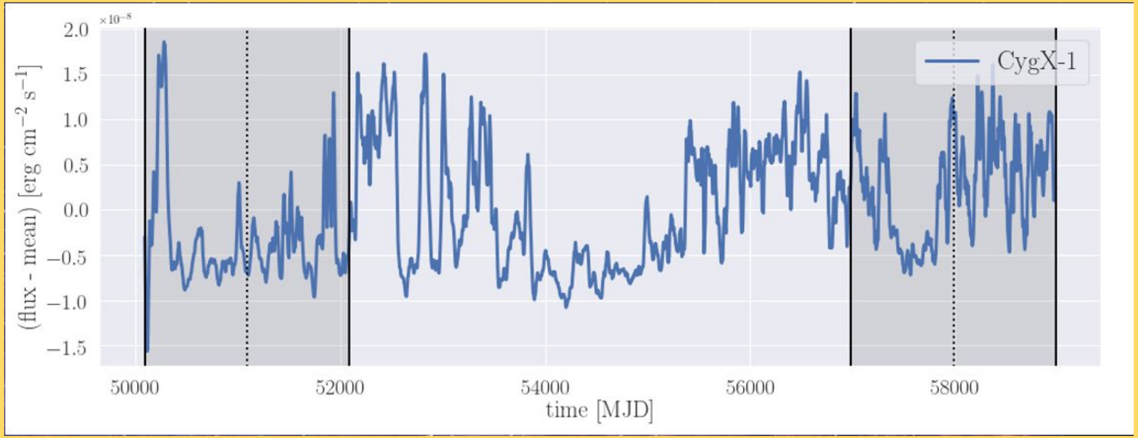

Data: 2-20 keV Flux, Rossi X-ray Timing Explorer (RXTE) All-sky Monitor (ASM) and MAXI

Cyg X-1: Known to undergo state changes regularly

Corona-dominated "hard" state: power-law energy spectrum (Comptonized), higher energy photons

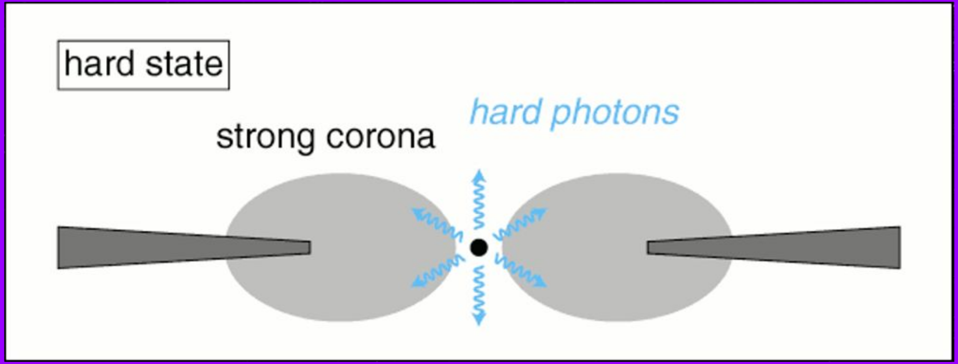

Accretion State Changes of Cyg X-1

Pointed observations (colored points) provide spectral classification (Γ_1)

Hardness-Intensity as a proxy for accretion state

Grinberg+2013

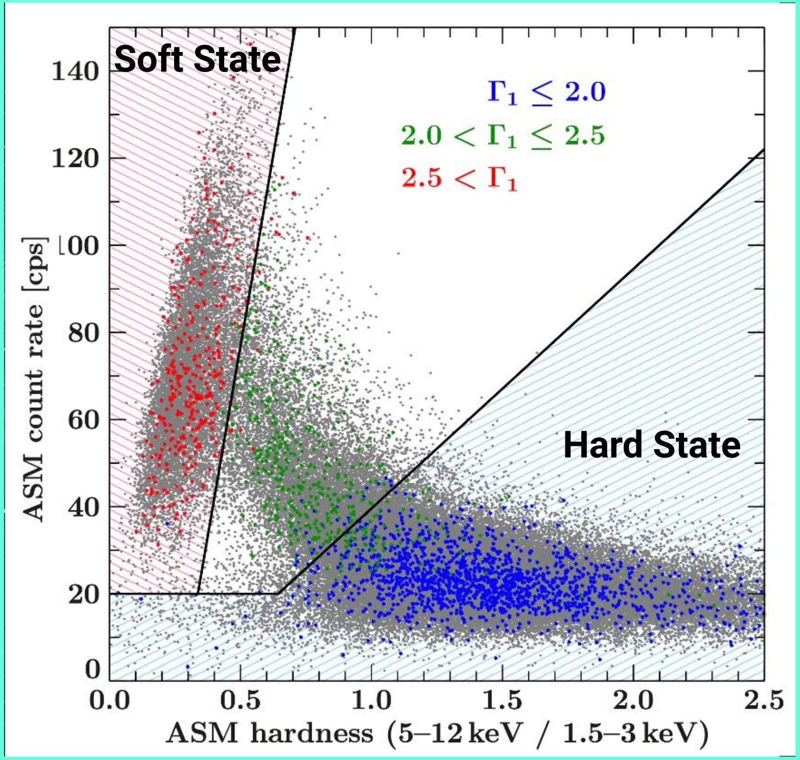

Accretion State Changes of Cyg X-1

Features from the RP:

DET: "Determinism" – proportion of points in RP that are part of diagonal lines

TT: "Trapping Time" – average length of vertical line

A total of 10 features

Broadbent & Phillipson 2023 (in review)

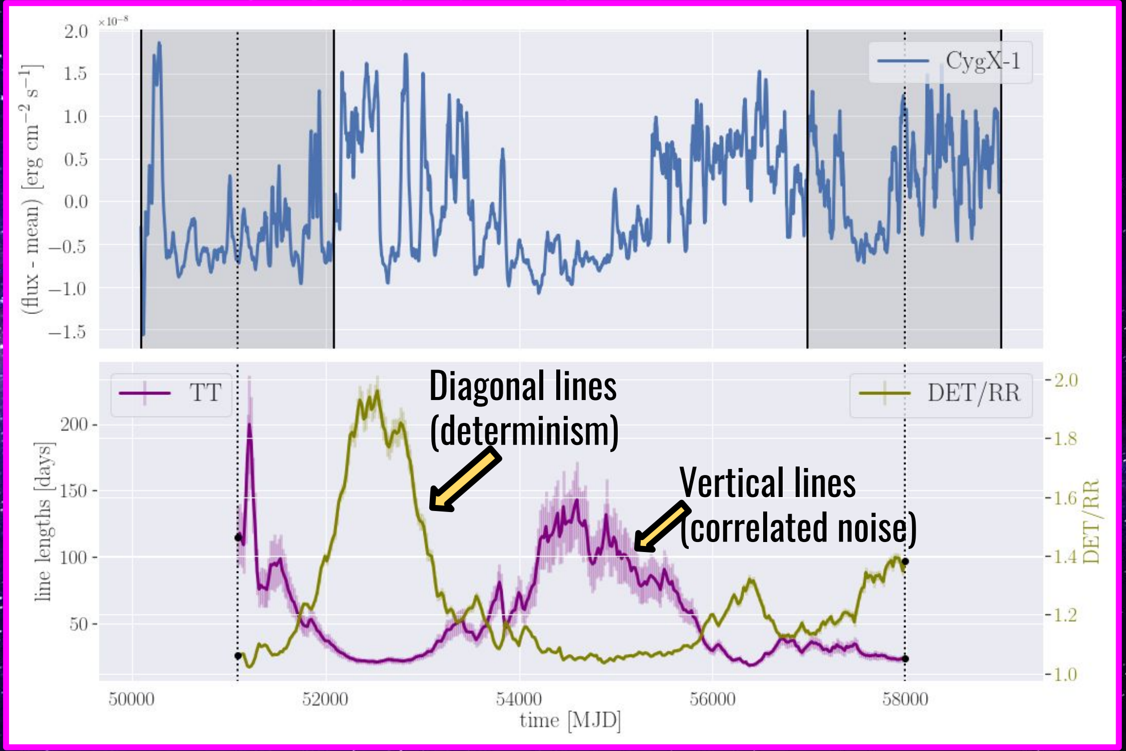

Changes in Variability States

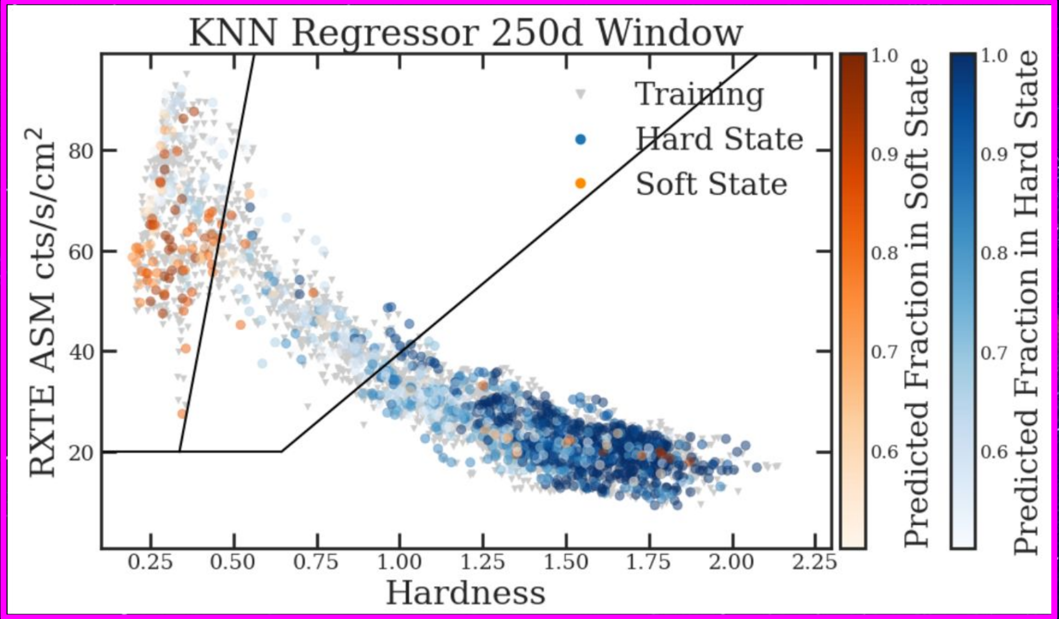

Broadbent & Phillipson 2023 (in review)

K-Nearest Neighbors Regression model:

- Use RP features as predictors and %RP in each spectral state as targets in training set
- Test on unlabeled data
- Predicts with up to 95% accuracy the state given **only** RP features

The Future

Pair Nonlinear Time Series Analysis with AI/ML Techniques

The Future

Pair Nonlinear Time Series Analysis with AI/ML Techniques

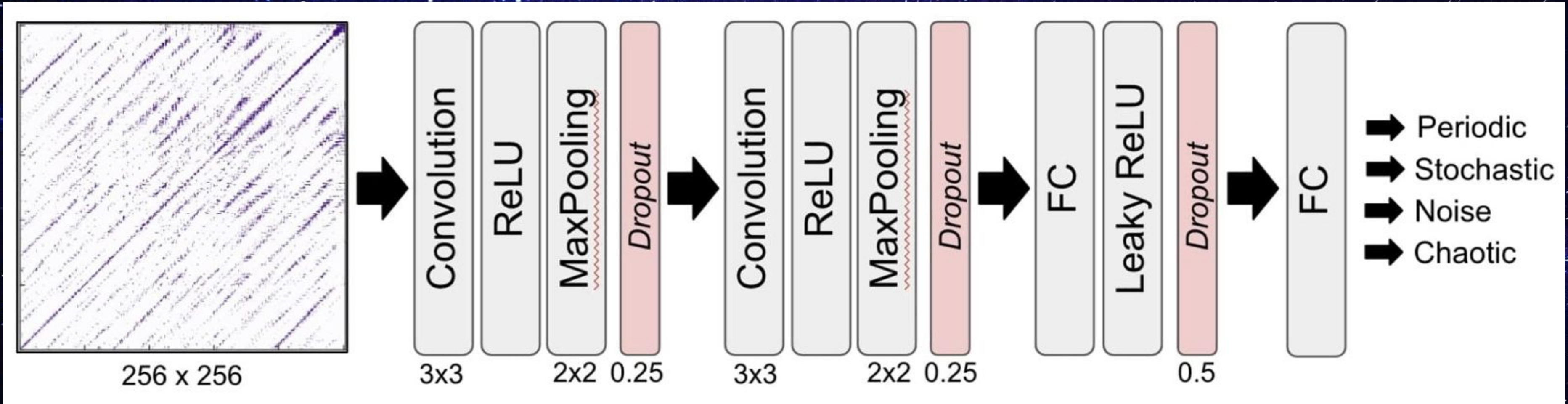

Use a Convolutional Neural Network to classify RPs of ZTF light curves into 4 dynamical classes

The Future

Pair Nonlinear Time Series Analysis with AI/ML Techniques

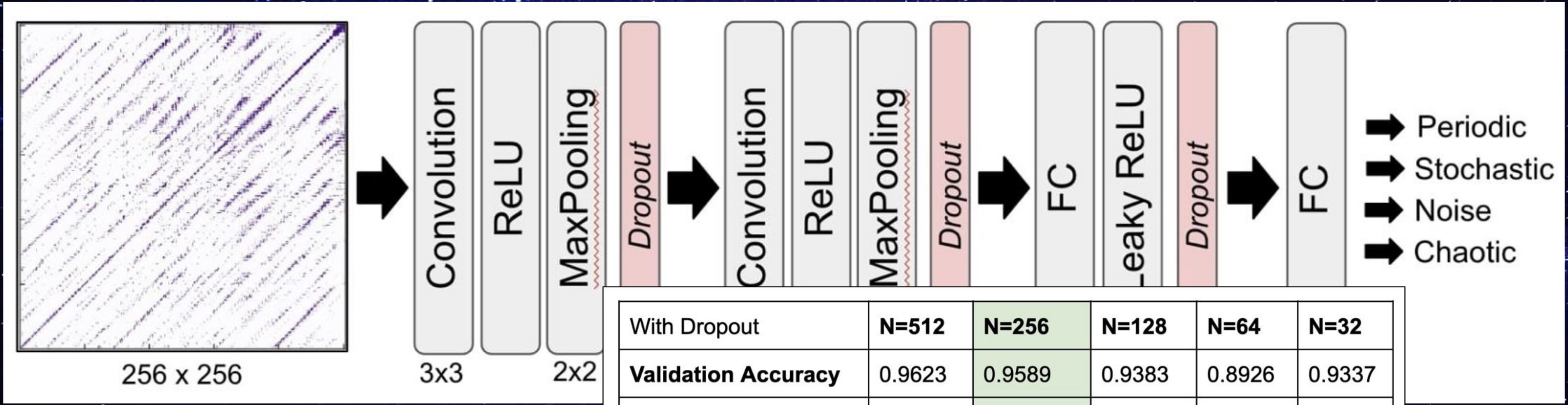

With Dropout	N=512	N=256	N=128	N=64	N=32
Validation Accuracy	0.9623	0.9589	0.9383	0.8926	0.9337
Validation Loss	0.1417	0.1297	0.1763	0.2798	0.2483

The Future

Pair Nonlinear Time Series Analysis with AI/ML Techniques

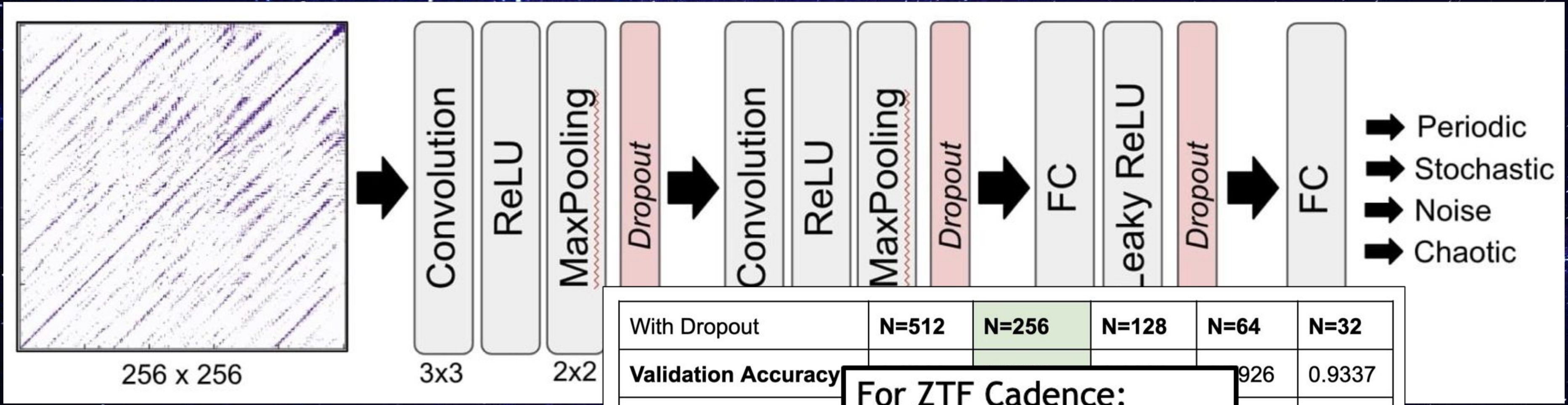

With Dropout	N=512	N=256	N=128	N=64	N=32
Validation Accuracy				926	0.9337
Validation Loss				798	0.2483

For ZTF Cadence:
Accuracy 77%
Loss 0.47

The Future

Pair Nonlinear Time Series Analysis with AI/ML Techniques

- Preliminary success with ZTF promises bright future with LSST

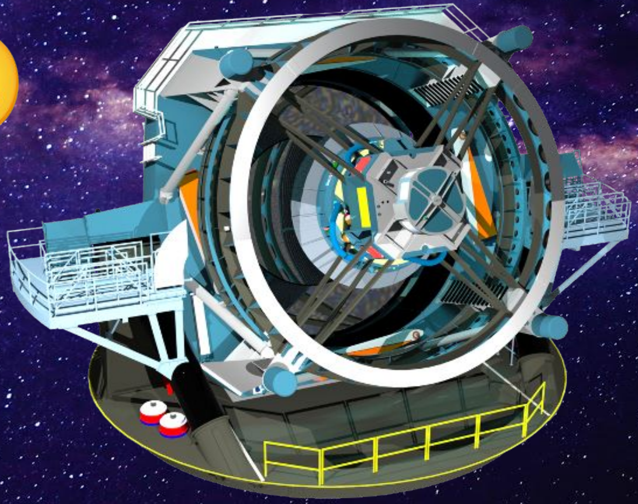

The Future

Revisit the data problems of traditional NLTS

Misra et al. 2004

The Future

Revisit the data problems of traditional NLTS

Dimension & Lyapunov exponent calculations:

- Require very long and detailed time series
- Very sensitive to noise

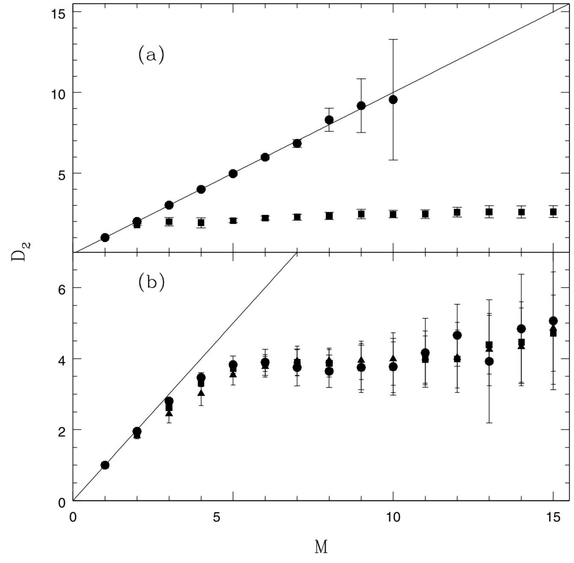

FIG. 1.—(*a*) D_2 vs. M for random points (*circles*) and for a Lorenz system (*squares*). For both curves the number of points used is 30,000, and the number of centers used in the computation is 2000. The straight line represents the $D_2 = M$ case, which is the expected result for random variation. (*b*) D_2 vs. M for GRS 1915+105 data obtained during class κ for three different values of the delay time: $\tau = 15$ s (*triangles*), 25 s (*squares*), and 100 s (*circles*).

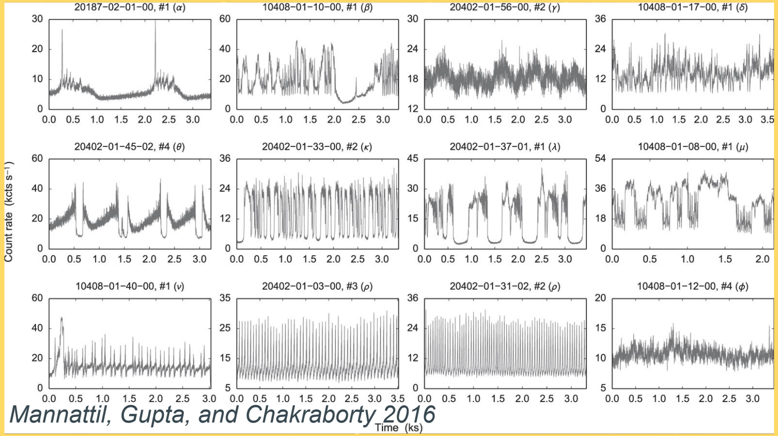

Mannattil, Gupta, and Chakraborty 2016

Correlation dimension, D: the rate at which the volume in M-dim space grows with radius R^M

Data limit: D ~ log(N)

Misra et al. 2004

The Future

Revisit the data problems of traditional NLTS

Dimension & Lyapunov exponent calculations:

- Require very long and detailed time series
- Very sensitive to noise

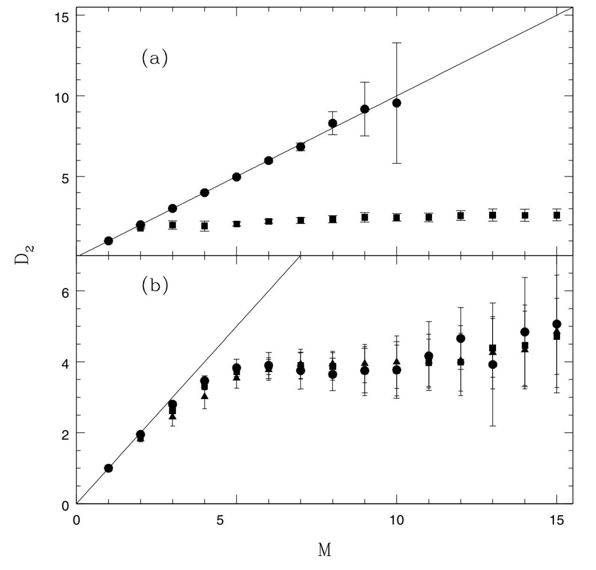

FIG. 1.—(*a*) D_2 vs. M for random points (*circles*) and for a Lorenz system (*squares*). For both curves the number of points used is 30,000, and the number of centers used in the computation is 2000. The straight line represents the $D_2 = M$ case, which is the expected result for random variation. (*b*) D_2 vs. M for GRS 1915+105 data obtained during class κ for three different values of the delay time: $\tau = 15$ s (*triangles*), 25 s (*squares*), and 100 s (*circles*).

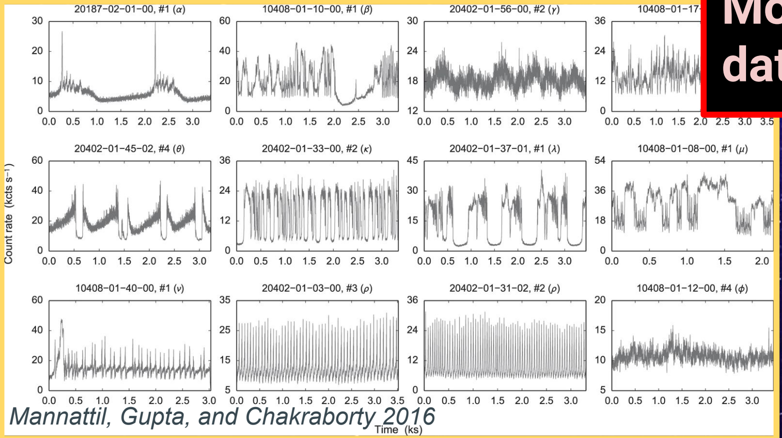

Mannattil, Gupta, and Chakraborty 2016

More high-quality data, please, thanks

Correlation Dimension, D: the rate at which the volume in M-dim space grows with radius R^M

Data limit: D ~ log(N)

The Future

https://strobe-x.org

Revisit the data problems of traditional NLTS

X-ray Probe Concept: STROBE-X

STROBE-X	RXTE/NICER
Wide Field Monitor (WFM) •Energy Range 2–50 keV •# of Camera Pairs: 4 •FOV/Camera Pair 70° × 70° FWHM •Energy Resolution 300 eV FWHM •Sky Coverage (Instantaneous) 4.1 sr •Angular Resolution 4.3 arcmin •Position Accuracy 1 arcmin •Sensitivity (1 s) 600 mcrab •Sensitivity (1 day) 2 mcrab	**All-Sky Monitor (ASM)** •Energy range: 2 - 10 keV •Time resolution: 80% of the sky every 90 minutes •Spatial resolution: 3' x 15' •Number of shadow cameras: 3, each with 6 x 90 degrees FOV •Collecting area: 90 square cm •Detector: Xenon proportional counter, position-sensitive •Sensitivity: 30 mCrab

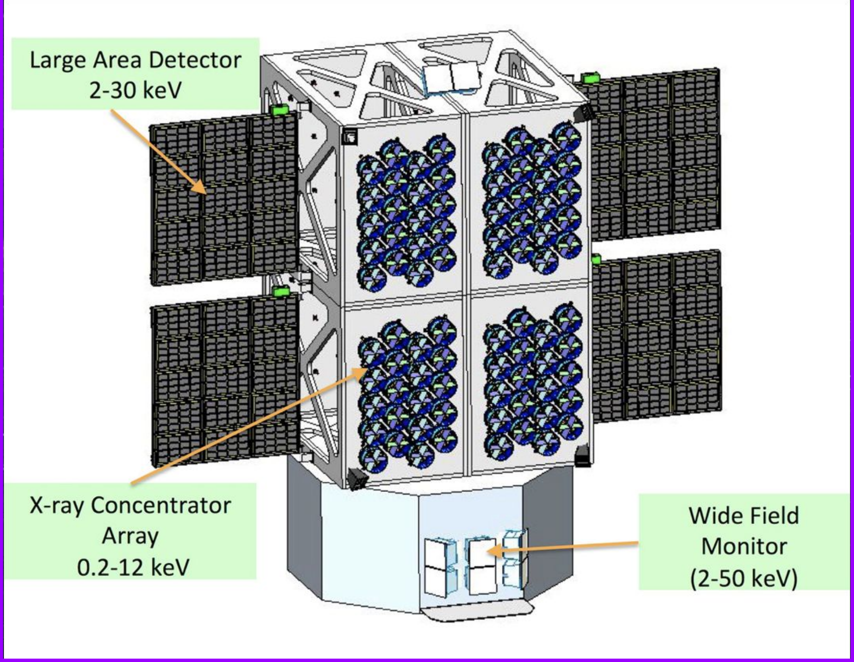

The Future

Revisit the data problems of traditional NLTS

STROBE-X and other X-ray satellites enable:

- Ensemble studies with X-ray light curves
- Correlations with accretion state and energy spectra
- Use bispectrum, RPs, and correlation dimension calculations alike

The Future

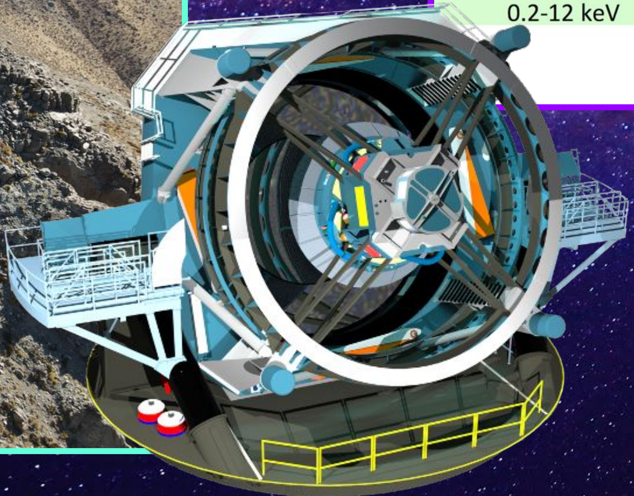

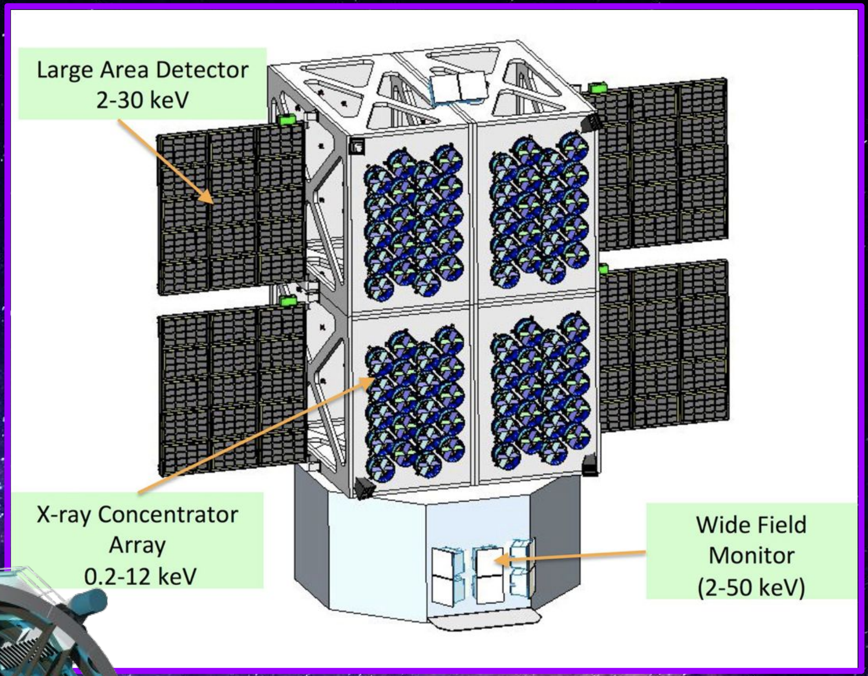
Large Area Detector
2-30 keV
X-ray Concentrator
Array
0.2-12 keV
Wide Field
Monitor
(2-50 keV)